ELSEVIER

Tectonophysics 255 (1996) 47–63

TECTONOPHYSICS

Subduction of diverging plates and the principles of slab window formation

Derek J. Thorkelson *

Earth Sciences Program, Simon Fraser University, Burnaby, B.C. V5A 1S6, Canada

Received 8 February 1995; accepted 19 July 1995

Abstract

Consumption of an ocean basin by subduction commonly brings a sea-floor-spreading ridge toward a deep-sea trench. If plate divergence and convergence continue after the ridge intersects the subduction zone, a slab window forms between the subducted parts of the diverging oceanic plates, producing anomalous thermal, physical and chemical effects in the surrounding asthenospheric mantle. In turn, these conditions alter the tectonic and magmatic evolution of the overriding plate, usually disturbing ordinary fore-arc and arc regimes. Differential lithospheric stresses on opposite sides of the triple junction contribute to disturbances in the overriding plate. Anomalous magmatism from fore arc to back arc may be accompanied by fore-arc metamorphism, strike-slip faulting, uplift, extension and, in extreme cases, rifting.

The shape and size of the window are controlled mainly by the pre-subduction ridge–transform–trench configuration, slab dip angles and vectors of plate convergence. Subducted ridge segments expand into windows whose margins approximately parallel the motion vectors between the triple junction and the subducting plates. Subducted transform faults continue to be active, usually as oblique-slip faults, until the plates separate. As transform faults subduct, they become longer on the plate which occupies the acute angle between ridge and trench, and shorter on the other plate. Trains of isolated windows produced by subduction of a segmented ridge–transform system progressively expand during descent, commonly merging together to form a *composite* slab window. Oblique subduction of a highly segmented ridge is likely to produce two or more *fraternal* slab windows, one at each site of ridge–trench intersection.

Above a slab window, arc volcanism diminishes and may be replaced by volcanism of mid-ocean ridge or rift affinity. The change in chemical character reflects various processes including elevated heat flow, decreasing hydration of the upper mantle, juxtaposition of supra- and sub-slab mantle reservoirs, asthenospheric upwelling and melting of the trailing plate edges. If the slab window migrates, the anomalous magmatic regime may be replaced by renewed arc volcanism. Identifying the effects of slab windows in ancient convergent margin assemblages requires an understanding of slab window principles and implications.

1. Introduction

Intersection of sea-floor-spreading ridges with subduction zones has been a topic of interest for over twenty-five years. Beginning with speculation that orogenesis in the western United States was caused by the North American plate overriding the East Pacific Rise (Palmer, 1968), studies of ridge–trench interaction have become increasingly sophisticated. DeLong and Fox (1977), Marshak and Karig (1977),

* E-Mail: dthorkel@sfu.ca.

SSDI 0040-1951(95)00106-9

DeLong et al. (1978) and Dixon and Farrar (1980) explored ideas suggested by Uyeda and Miyashiro (1974) on the thermal, magmatic and tectonic aspects of overridden spreading ridges. In a landmark paper, Dickinson and Snyder (1979) developed these ideas and showed that a subducting ridge will evolve into an ever-widening gap between the downgoing oceanic slabs: a slab window. Since then, numerous papers have corroborated their findings, and elaborated on the magmatic and tectonic effects related to this important geological phenomenon (Sisson et al., 1994). Despite the geological importance of ridge–trench interactions, many geologists are not familiar with the mechanics and implications of slab window formation.

This paper outlines the salient factors influencing ridge–trench intersections and slab window geometry. Idealized slab windows are constructed for a variety of ridge–trench configurations, slab dip angles and plate kinematics. Implications are considered for the mantle, and magmatism in the overriding plate. The analysis shows that slab window formation and migration may be the cause of tectonic and magmatic anomalies in ancient convergent margins.

2. Do spreading ridges subduct?

Ocean floors grow at spreading ridges and are consumed in subduction zones. Both processes commonly occur in the same ocean basin (e.g., Pacific, Atlantic, Mediterranean, Indian). Plate growth is approximately symmetrical, whereas subduction of ocean floor occurs at some angle to the axis of growth, and causes asymmetrical basin consumption. Consequently, the process of subduction tends to bring spreading ridges toward subduction zones.

The age, thickness and density of oceanic lithosphere decreases toward spreading ridges. As a spreading ridge approaches a trench, the buoyancy of the subducting slab increases. Relative to the asthenosphere, oceanic lithosphere older than about 10 Ma is negatively buoyant and inherently subductable, whereas lithosphere younger than about 10 Ma is positively buoyant (Cloos, 1993). The width of buoyant lithosphere bounding a spreading ridge depends on the rate of spreading. For example, a spreading ridge with a half-spreading rate of 25 km/Ma will be bounded by about 250 km of buoyant lithosphere. However, all but the youngest parts of this lithosphere (< 2 Ma; 50 km wide) will become negatively buoyant during subduction because of progressive metamorphism to amphibolite and eclogite, and will thereby contribute to the force of slab pull (Cloos, 1993).

Empirical and theoretical studies show that subduction of progressively younger lithosphere will tend to cause shallowing of subduction angles and reduction in subduction rates (e.g., Cross and Pilger, 1982; Larter and Barker, 1991; Cloos, 1993). In some cases, subduction may stop before the ridge intersects the trench, leading to possible cessation of sea-floor spreading. This situation appears to have developed along parts of the East Pacific Rise where it approached North America in the middle Tertiary [see alternative view by Dixon and Farrar (1980) and Farrar and Dixon (1993)]. Fossil spreading ridges are preserved in the oceanic crust off the shore of California and Mexico (Atwater and Severinghaus, 1989), suggesting that ridge–trench intersection did not occur in that region. Instead, spreading ceased and the buoyant parts of the subducting plate broke up into nonsubducting microplates with independent kinematics. In other cases, however, subduction is uninterrupted and even the youngest parts of the oceanic plates are drawn into the trench. In these situations, commonly referred to as "ridge subduction", the newly formed trailing edge of one or both of the diverging oceanic plates descends into the asthenosphere. For this to occur, the combined forces of ridge push and slab pull must exceed the buoyant force exerted by the ridge-proximal part of the plate (Larter and Barker, 1991). In addition, the strength of the plate must be sufficient for the slab to subduct without fragmenting (Van den Beukel, 1990). Apparently these conditions were satisfied in several Cenozoic ridge–trench encounters along the coasts of North America (Thorkelson and Taylor, 1989), Chile (Herron et al., 1981; Forsythe and Nelson, 1985), the Antarctic Peninsula (Hole, 1988), the Solomon Islands (Weissel et al., 1982; Johnson et al., 1987) and Japan (Hibbard and Karig, 1990).

3. Slab window formation

3.1. Unzipping the divergent plate boundary

At a ridge–trench encounter, the trailing edge of one or both of the diverging oceanic plates descends into and becomes surrounded by hot mantle. Even if subduction is nearly horizontal, as in the Late Cretaceous beneath the western United States (Dickinson and Snyder, 1978; Bird, 1988), the slab is likely to be separated from the overriding plate by a wedge of asthenosphere (Livaccari and Perry, 1993). Although magma may continue to form between the diverging plates, it will not cool sufficiently to solidify onto the trailing plate edges (Dickinson and Snyder, 1979), which become hot and begin to melt (Severinghaus and Atwater, 1990; Peacock, 1993). Rather, any magma generated will rise through the asthenosphere between the trailing slab edges and pool beneath or ascend into the overriding plate. Consequently, plate growth along the trailing slab edges will cease, and a gap, or slab window, will form between them. Plate divergence in this no-growth environment results in progressive unzipping of the ridge–transform plate boundary.

3.2. Factors affecting window geometry

In this paper, slab window geometries are modelled assuming that subduction occurs continuously and plate continuity is unbroken. Under these conditions, the shape of a slab window is dependent on three main factors (Dickinson and Snyder, 1979; Thorkelson and Taylor, 1989): (1) relative plate motions; (2) pre-subduction ridge–transform fault configuration; and (3) subduction angles. In addition, window size and shape are modified by thermal erosion (e.g., McKenzie, 1969; Severinghaus and Atwater, 1990; Kay et al., 1993), deformation caused by spherical shell stress (Yamaoka and Fukao, 1986) and lateral or downdip changes in slab dip angles (Dickinson and Snyder, 1979; Cross and Pilger, 1982; Thorkelson and Taylor, 1989). Of these, thermal erosion (melting and assimilation of the window edges) is probably the most important, resulting in progressive widening of the slab window with depth. Spherical shell strain, a consequence of decreasing Earth volume with increasing depth, tends to narrow the window, and may partially compensate for the effects of thermal erosion. The degree to which spherical shell strain counterbalances thermal erosion depends on factors such as divergence rate (rapid divergence favours thermal erosion), convergence rate (slow convergence favours thermal erosion), angle of ridge–trench intersection (higher angle favours greater spherical-shell-induced narrowing), and slab dip angles (steep angles of descent may correspond with greater spherical shell strain). Lateral or downdip changes in slab dip may occur because the parts of the slabs forming the window margins are young, hot and buoyant, and may curl upward.

Slab window geometries using two types of diagrams are illustrated in Figs. 1–8. One represents the plates in plan view (plane space), and the other represents relative plate motions by vectors in velocity space (McKenzie and Morgan, 1969). The figures progress from simple to complex geometries, concluding with a "general case" window (Fig. 8b and Fig. 9). Sea-floor spreading is symmetrical, and plate motions are uniform. Thermal erosion, spherical shell strain and upcurling of the window margins are not considered.

3.3. Windows between horizontally subducting slabs

In Figs. 1–5, subduction is horizontal (dip angle of each slab is 0°) in order to illustrate how window shape is largely controlled by relative plate motions and ridge–transform fault configurations. During "flat" subduction, the margins of a slab window are parallel to the vectors between the triple junction (J) and the oceanic plates (B and C), drawn relative to the overriding plate (A). The predicted shape of a window is therefore similar to the shaded triangle in the velocity diagram, with apices at J, B and C (cf. Dickinson and Snyder, 1979). These figures are applicable to slab windows formed during shallow subduction, such as the postulated Kula–Farallon slab window beneath the western United States in Late Cretaceous times (Thorkelson and Taylor, 1989; Babcock et al., 1992), when subduction was nearly horizontal (Dickinson and Snyder, 1978).

If the triple junction does not migrate (i.e., A = J in velocity space), then the window margins will be parallel to the vectors of convergence (Fig. 1). In the

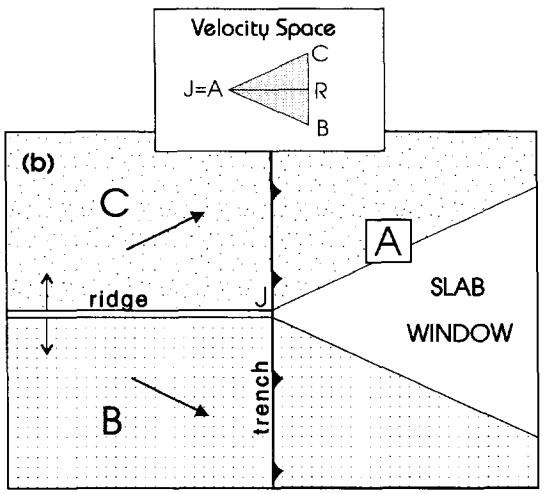

Fig. 1. Slab window formed by orthogonal intersection between a spreading ridge and a trench. Two diverging oceanic plates (*B* and *C*) are subducting horizontally beneath an overriding plate (*A*). Arrows on plates *B* and *C* indicate the velocities of convergence with reference to plate *A*. Subducted parts of plates *B* and *C* are projected upward to the surface of the overriding plate. In the velocity diagram (inset), relative motions are provided for plates *A*, *B* and *C*, the spreading ridge (*R*) and the triple junction (*J*). The triple junction is located at the intersection between a line oriented parallel to the trench passing through *A*, and a line normal to vector *BC* containing point *R*. Vectors *AB* and *AC* are equivalent to the convergent vectors shown in plane space. The shaded triangle *JBC* is similar to the shape of the slab window.

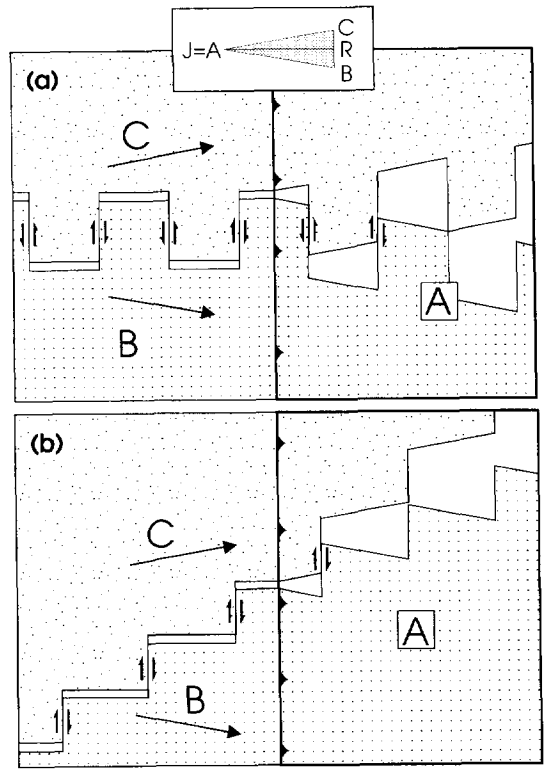

Fig. 2. Slab window formed by orthogonal subduction of segmented ridge–transform systems. Relative to Fig. 1, the angle between the vectors of plate convergence (*AB* and *AC*) is smaller, yielding narrower slab windows. In (a) the ridge is segmented by alternately left- and right-stepping transform faults, whereas in (b) the transforms are consistently left stepping. In both cases, individual slab windows have formed at the trench, expanded and merged with earlier-formed windows to form *composite* slab windows.

plate diagram, ridge and trench are perpendicular and angles of convergence are symmetrical about the ridge. The subducted parts of plates B and C are projected vertically to the surface. The trailing edges of the subducted slabs are parallel to vectors AB and AC in the velocity diagram. The V-shaped region between the subducted plate edges is the slab window, a gap occupied by asthenospheric mantle. The window has this shape because points on plates B and C, originating at the triple junction, diverge as they move beneath plate A. The divergence between the subducted slabs (vector BC) is accompanied by flow of asthenosphere into the window.

In Fig. 2, the spreading ridge is segmented by transform faults, leading to an uneven window margin. In velocity space, the triple junction is coincident with plate A, indicating that the ridge–trench intersection will not migrate. During the subduction of each ridge segment, the triple junction remains fixed at one location at the trench. When a transform fault intersects the trench, the triple junction "jumps" along the trench to the locus of the next trench–ridge segment intersection.

In Fig. 2a, the ridge is offset by alternately left- and right-stepping transforms, whereas in Fig. 2b, the transforms are consistently left stepping. As each ridge segment is overridden, a slab window is generated, with margins parallel to the convergent plate vectors. As each transform is subducted, a new triangular-shaped window begins to form from the new triple junction. The transform faults maintain their orientation after subduction, and continue to be active until the amount of plate separation exceeds transform length. As the slabs diverge, windows

separated by transform faults merge resulting in progressive growth of a *composite* slab window with zipper-shaped margins.

If the triple junction migrates (A is not coincident with J in velocity space), then the window margins are not controlled simply by the angles of convergence (Fig. 3). Rather, the shape of the window reflects synchronous plate convergence and triple junction migration, and the window margins will be parallel to velocity vectors JB and JC. The ridge is oriented at 45° to the trench, and the triple junction is moving southward along plate A, according to vector AJ (Fig. 3a). Window geometry is constructed by vectors on the plate diagram for two increments of time (Fig. 3b, c). In Fig. 3d is shown that the slab window has a southwesterly tapering V-shape and is migrating southward beneath the overriding plate.

Subducting transform faults which are not parallel to the trench change in length as they subduct (Fig. 4). In this example, the diverging plates are separated by a right-stepping ridge–transform system, and have the same relative plate motions as in Fig. 3. The subducting transform faults decrease in length on one plate but increase on the other, forming steps of unequal length in the opposing window margins. The longer steps develop on the plate which occupies the acute angle between ridge and trench (plate B).

The amount of growth or shrinkage of a transform boundary during subduction depends on the length of time required to subduct the transform. A transform fault oriented at a high angle to the trench tends to undergo greater change in length than a fault oriented at a low angle to the trench. Where a transform fault is parallel to the trench (Fig. 2), subduction of the entire fault will occur at one "moment" in time, and no change in length will occur.

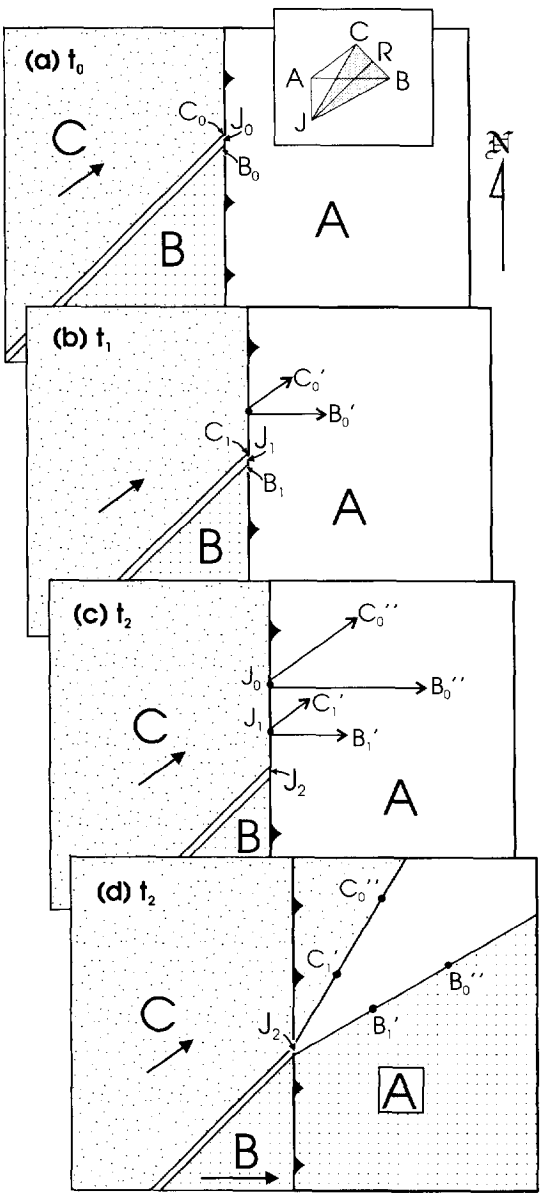

Fig. 3. Construction of a slab window produced by non-orthogonal intersection between ridge and trench, demonstrating that window shape is determined by the vectors between the triple junction and the subducting plates (*JB* and *JC*). Slabs are subducting horizontally. In (a) time = t_0, and the ridge–trench intersection is at position J_0. At time = t_1 (b), the triple junction has migrated to point J_1, and the parts of plates *B* and *C* which were at triple junction J_0 (B_0 and C_0) have subducted beneath plate *A* to points B_0' and C_0'. At time = t_2 (c), the triple junction has migrated to point J_2, points B_0 and C_0 have subducted one vector length farther to new positions B_0'' and C_0'', and the parts of plates *B* and *C* which were at triple junction J_1 (B_1 and C_1) have subducted to points B_1' and C_1'. At this time, the window margins can be visualized by connecting point J_2, from which the window must emanate, to points B_0' and B_1' along the trailing edge of subducted slab *B*, and to points C_0'' and C_1' along the trailing edge of slab *C*. This procedure has been followed in (d), which illustrates the southwesterly tapering slab window, filled by asthenospheric mantle.

If one of the diverging plates (C) is moving parallel to the trench (Fig. 5), then slab window formation is accompanied by development of a strike-slip plate boundary (AC). The diagram also indicates how multiple slab windows may form concurrently from subduction of a segmented ridge. As the trailing edge of plate B is dragged beneath plate A, a triangular slab window forms at each locus of intersection. As subduction proceeds, these *fraternal* slab windows grow and eventually eventually merge into a single, composite window underlying the entire leading edge of plate A. Fraternal windows are most likely to occur where ridge and trench are nearly parallel, and transform faults step "back" toward the trench.

If ridge and trench are nearly parallel (e.g., southern Chile, Antarctic Peninsula) window shape is likely to depart from predicted window geometry because a large area of newly formed oceanic lithosphere simultaneously approaches the trench. As the ridge approaches the trench, the newly formed lithosphere of the inboard converging plate (plate B in Fig. 5) becomes progressively more resistant to subduction, and is likely to become fragmented into microplates with independent kinematics (cf. Riddihough, 1984; Stock and Molnar, 1988), producing more complex window shapes. As noted by Cande et al. (1987), plate fragmentation and "pivoting subduction" (Menard, 1978) is likely to be greatest where transform faults step "back" toward the trench (Fig. 5), as in the encounter between North America and the East Pacific Rise (Atwater, 1970). Fragmentation is least where transform faults consistently step "away" from the trench, as in the Antarctica–Phoenix and South America–Chile Rise collisions

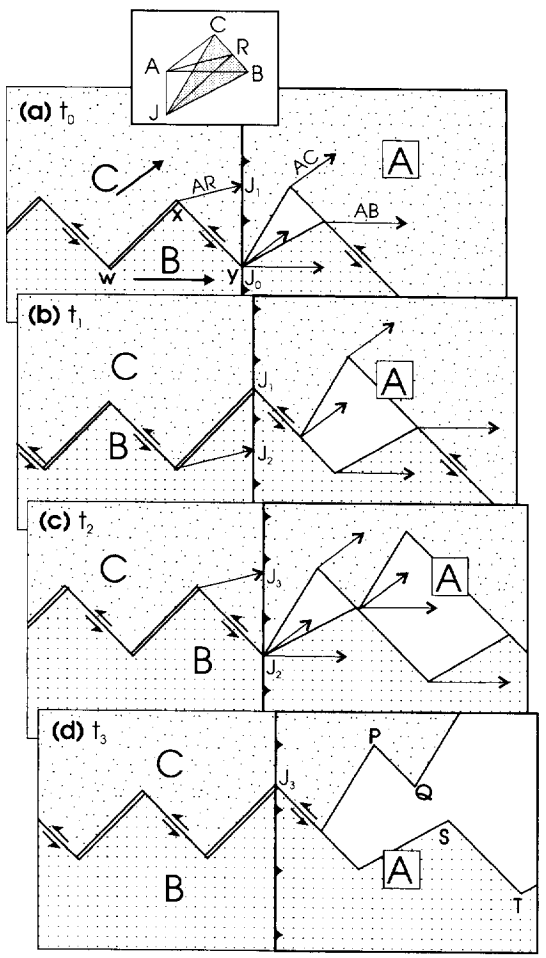

Fig. 4. Construction of a slab window formed by non-orthogonal intersection between a trench and a segmented ridge–transform system. As the transform faults subduct, they become steps of unequal length in the opposing slab window margins. (a) to (d) show the evolution of the slab window for three increments of time. Vectors in each figure are used to construct window geometry in successive frames. In (a) (time = t_0), a triangular slab window has formed from subduction of a long transform fault followed by a ridge segment. The window margins are parallel to vectors *JB* and *JC* in the velocity diagram. The next part of the divergent plate boundary to be subducted is transform fault *XY*. (b) ($t = t_1$) shows the plate configuration after subduction of transform *XY*. During the time interval t_0 to t_1, points on plates *B* and *C* which were at triple junction J_0 moved according to vectors *AB* and *AC*, respectively, and became separated from one another by an amount equivalent to vector *BC*. As plates *B* and *C* diverged, the subducted part of plate *C* moved toward the next ridge segment to be subducted (*WX*), whereas the subducted part of plate *B* moved away from ridge segment *WX*. Therefore, the step in the margin of plate *C* produced by subduction of transform *XY shrank* in length, whereas the opposing step in plate *B grew* in length. The amount of shrinkage of the step in plate *C* equals the amount of growth of the step in plate *B*, which equals the amount of half-spreading during this interval of time. The amounts of shrinkage and growth sum to the amount of window expansion, which is equal to the amount of full spreading given by vector *BC*. In (c) ($t = t_2$), the first window has expanded and a second window has grown during subduction of ridge segment *WX*. In (d) ($t = t_3$), the two windows have merged to form a composite slab window. The steps in the window margin produced by subduction of transform *XY* are shown as unequal window edges *PQ* on plate *C* and *ST* on plate *B*.

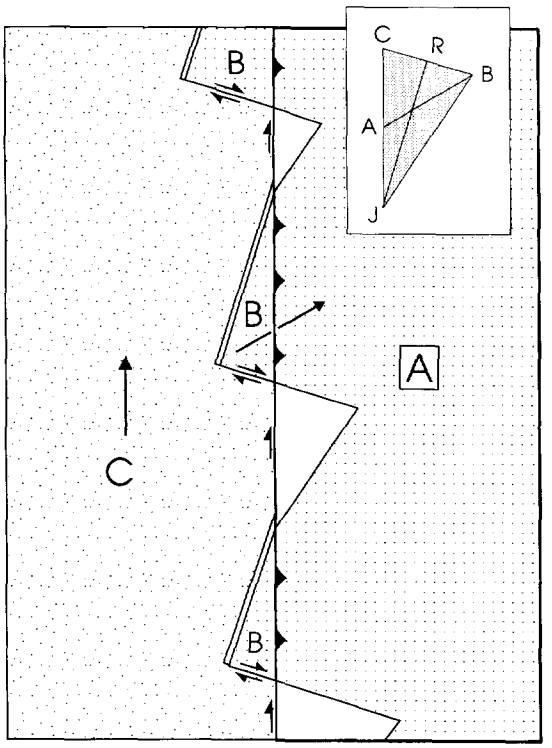

Fig. 5. Development of *fraternal* slab windows from low-angle convergence between trench and a highly segmented ridge–transform system. The motion of plate *C* with reference to plate *A* is parallel to the trench. As each ridge segment is subducted, the trench is progressively converted to a strike-slip fault between plates *A* and *C*, and a slab window forms where the trailing edge of plate *B* slides beneath plate *A*.

(Larter and Barker, 1991; Forsythe and Nelson, 1985). Thermal erosion of plates with back-stepping transforms (Fig. 5) will significantly modify the shape and size of the slab window, producing a gap between the diverging plates even if subduction stalls and the spreading ridge does not subduct (Severinghaus and Atwater, 1990). If the second oceanic plate to arrive at the trench has a component of divergence with reference to the overriding plate (e.g., if vector AC in Fig. 5 was west of north), then the second oceanic plate may undergo "secondary spreading", probably at an angle to the original axis of spreading (Farrar and Dixon, 1993). Alternatively, the overriding plate may become extended (Farrar and Dixon, 1993; Luyendyk, 1995).

3.4. Windows between dipping slabs

The effect of slab dip on window geometry is illustrated in Figs. 6–8. Surface projections of slab windows are indicated for dip angles varying from 0 to 75°. Points on the slab edges forming the window margins shift trenchward with increasing slab dip (cf. Dickinson and Snyder, 1979). For uniform slab dip angles, the distance from the trench of a given point on a slab is calculated as: $\text{distance}_{\text{dipping slab}} = \text{distance}_{\text{horizontal slab}} \times \cos(\text{dip angle})$. As indicated in both Figs. 6 and 7 the position of the window margin is adjusted trenchward by 13% for slabs dipping at 30°, by 50% for 60° dip, and by 74% for 75° dip. In Fig. 6, the plate configuration and motions are equivalent to those in Fig. 1, such that the shape of the slab window at 0° dip is identical to that in Fig. 1. For progressively steeper slab dips, points on the window margins are progressively closer to the trench, producing a wider surface projection. In Fig. 7, the projected area of the window becomes progressively smaller at higher dip angles.

Window shape will be affected by slabs dipping at different angles (Fig. 8). In Fig. 8a, a composite window has formed from horizontal subduction of a right-stepping ridge–transform system. As time passes, windows will continue to bud from each new

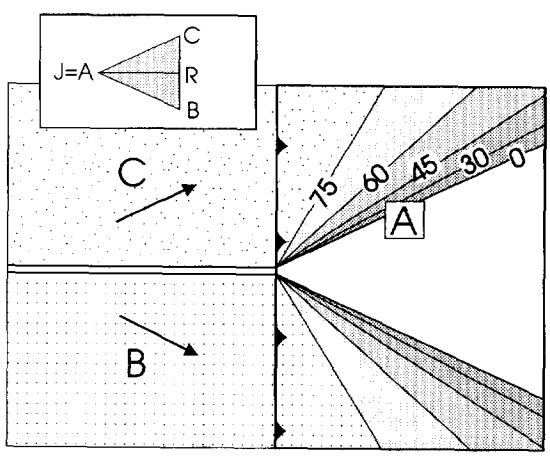

Fig. 6. The effect of slab dip on surface projection of slab window formed by orthogonal intersection between ridge and trench (cf. Fig. 1). As dip angle increases, the window margins retreat trenchward, progressively widening. At 30° dip, trenchward adjustment is only 13%, whereas at 60° dip, adjustment is 50%.

ridge–trench–trench triple junction, merge with earlier-formed windows, and migrate southward. In Fig. 8b, the subducted slabs descend into the asthenosphere at different dip angles. Plate B ("leading plate") descends at 25°, whereas Plate C ("trailing plate"), which is converging more slowly and less orthogonally, descends more steeply at 50° (cf. Isacks and Barazangi, 1977; Cross and Pilger, 1982). The surface projection of the dip-modified window is wider and less symmetrical than the horizontal window in Fig. 8a. The window illustrated in Fig. 8b is a "general case" window, formed where: (1) the ridge and the trench are converging obliquely; (2) the ridge is segmented by transform faults; (3) one of the slabs dips more steeply than the other; and (4) the axis and width of arc volcanism are different on opposite sides of the window.

A block diagram of a slab window similar to that in Fig. 8b illustrating non-orthogonal subduction of an alternately left- and right-stepping ridge–transform system (Thorkelson, 1990) is presented in Fig. 9. The diverging slabs are subducting at different rates, and at different angles of dip. The small, triangular window adjoining the spreading ridge is separated from a larger, composite slab window by a subducted transform fault. After its subduction, this transform fault became an oblique-slip fault to accommodate both divergence and differential tilting caused by the contrasting angles of slab descent. A

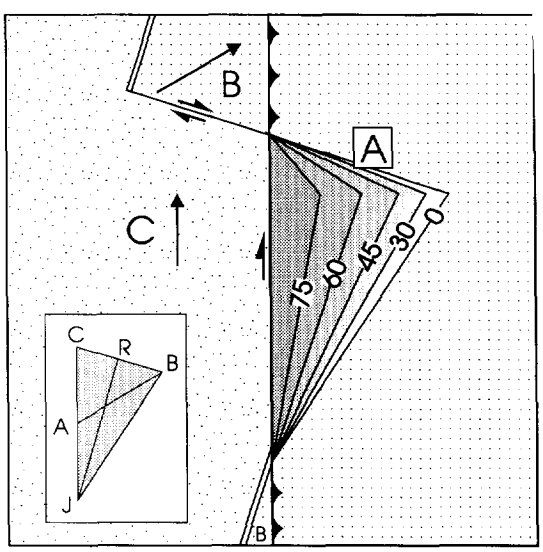

Fig. 7. Illustration of the effect of slab dip on window geometry where one of the diverging plates (plate *C*) is moving parallel to the trench, and the other is being subducted (cf. Fig. 5). With increasing dip angles, the surface projection of the window becomes progressively smaller.

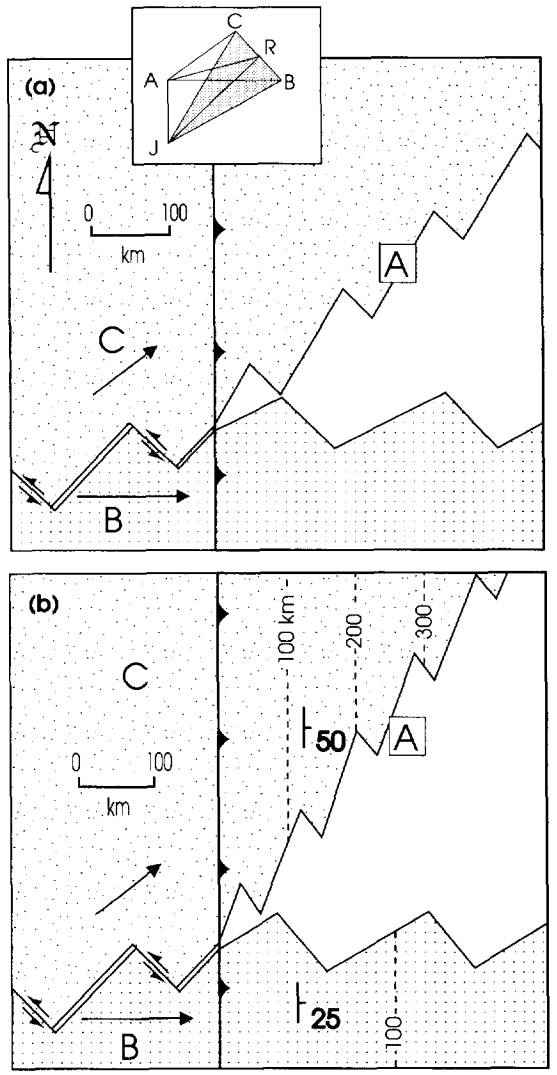

Fig. 8. Comparison of slab window surface projections illustrating the effect of different slab dip angles. In (a), the slabs are subducting horizontally, whereas in (b) plate *B* is descending at 25°, and plate *C* at 50°. In (b), points on the window margin of slab *B* have been adjusted toward the trench from the position in (a) by 9%; points on the margin of slab *C* have been adjusted by 36%. Depth contours at 100 km intervals for the upper surfaces of the slabs are indicated by dashed lines.

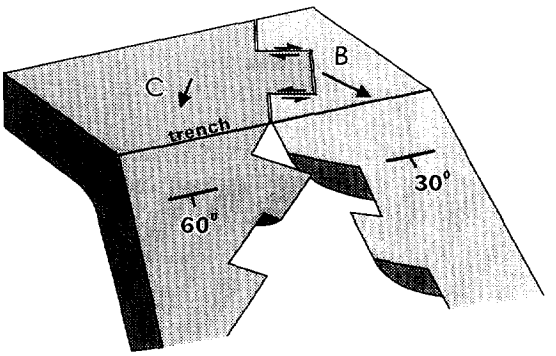

Fig. 9. Block diagram of a composite slab window formed by non-orthogonal subduction of an alternately left- and right-stepping ridge–transform system. Angle between ridge and trench is 60°. Convergence vectors on sea floor indicate plate *B* is subducting more rapidly than plate *C*; correspondingly, plate *B* dips at 30°, whereas plate *C* dips more steeply at 60°. As transform faults subduct, they change from strike-slip faults to oblique-slip faults to accommodate both divergence and differential tilting. The former transform parts of the window margin on slab *B* are longer than corresponding edges on plate *C* because plate *B* occupies the acute angle between ridge and trench.

similar window between slabs of equal dip is modelled in the context of slab–lower mantle interaction in Fig. 10 (Thorkelson, 1994). The window is bounded by slabs extending to and along the top of highly viscous lower mantle at about 660 km depth (Irifune and Ringwood, 1993; Gasparik, 1993). At subduction rates of 5–10 cm/a, the slabs could have reached this depth after 10–20 Ma of subduction. This style of slab–mantle interaction, in which slab continuity is maintained and the lower mantle acts as a barrier to descending slabs, is permissive according to studies of seismic tomography, mantle rheology and chemistry (Thompson et al., 1984; Zhou, 1990; Van der Hilst et al., 1991; Van der Hilst and Seno, 1993; Irifune and Ringwood, 1993; Gasparik, 1993). As with all slab windows, the one in Fig. 10 is the locus of chemical and thermal anomalies and is a potential pathway for asthenospheric flow which would otherwise be blocked by the descending oceanic slabs. The fore-arc to retro-arc distribution of active slab window-related volcanoes (black) be-

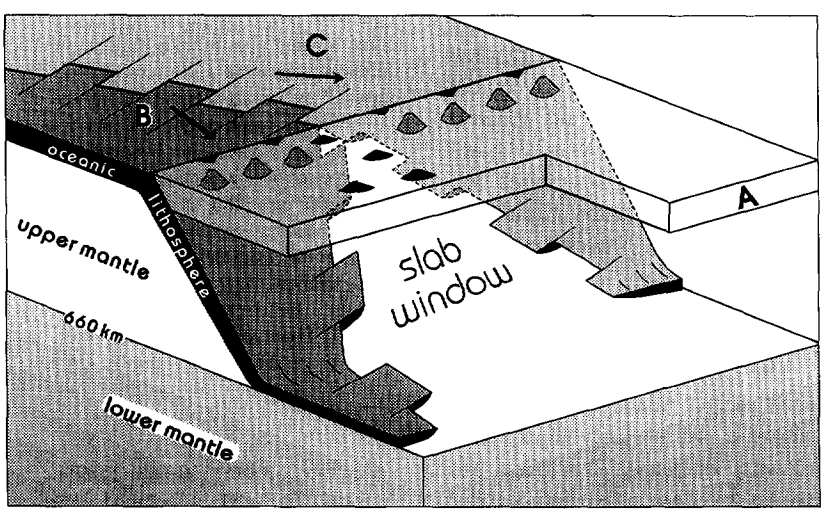

Fig. 10. Schematic block diagram of a slab window between two subducting oceanic plates (Thorkelson, 1994). The sea-floor-spreading ridge, segmented by alternately right- and left-stepping transform faults, is converging with the trench at a 75° angle. The transform fault offsets on the window margin of plate *B* are longer than on plate *C* because plate *B* occupies the acute angle between ridge and trench. The slabs are descending at 45° through the upper mantle, then sliding along the top of lower mantle. Oceanic plates *B* and *C* are converging according to the convergent plate vectors (arrows). Plate *B*, converging more orthogonally and subducting more rapidly than plate *C*, reached the 660 km discontinuity prior to plate *C*. On overriding plate *A*, calc-alkaline volcanoes (grey) form a volcanic arc, while tholeiitic to alkalic volcanoes (black) are active above the general region of the slab window. Diagram is drawn in orthographic space, and neglects probable spherical shell strain, thermal erosion, and variable slab dip angles.

tween flanking arc volcanoes (grey) is broadly based on Patagonia where patterns of late Tertiary magmatism are largely controlled by slab window formation and migration (Forsythe and Prior, 1992).

4. Magmatism and the mantle

4.1. Thermal, chemical and physical considerations

Slab window formation affects the mantle and magmatism in the overriding plate. Asthenosphere above a slab is cooled by transfer of heat to the cold downgoing slab (McKenzie, 1969), and is hydrated by water released from the slab as it undergoes metamorphism to eclogite (Gill, 1981; Peacock, 1993). Asthenosphere beneath a slab is little affected by either process, and remains relatively hot and dry. In a slab window, supra-slab asthenosphere is placed in direct contact with sub-slab asthenosphere (Fig. 11). Above the window, hydration of asthenosphere ceases and heat flows upward from hotter sub-slab mantle into the supra-slab mantle reservoir.

Two principal changes to the mantle occur as a slab window develops: a decrease in hydration and an increase in temperature (DeLong et al., 1979). These changes result in both chemical and thermal anomalies in the upper mantle beneath convergent margins. The anomalies will tend to be greatest where subduction is shallow and the overlying mantle wedge is thin. The location of the anomalies will be blurred to some degree by mantle circulation induced by slab motion (Davies and Stevenson, 1992; Peacock, 1993).

Arc volcanism, a normal consequence of subduction, results mainly from hydration of the mantle wedge (Gill, 1981). The calc-alkaline compositions which typify arc rocks reflect this hydrous source. Reduced hydration above a slab window causes normal arc volcanism to wane or cease. This effect has been noted in California by Dickinson and Snyder (1979) and Johnson and O'Neil (1984), in the Antarctic Peninsula by Hole et al. (1995), in British Columbia by Bevier et al. (1979) and Thorkelson and Taylor (1989) and in Chile by Ramos and Kay (1992). Tholeiitic to alkalic magmatism may supplant calc-alkaline magmatism in the region of the slab window (e.g., Marshak and Karig, 1977; Hole et al., 1991; Forsythe and Prior, 1992; Cole and Basu, 1995). The slab-window-related magmatism may result from various processes, including mantle currents, heating of the mantle wedge, mixing between sub-slab and supra-slab mantle reservoirs, partial melting of the trailing plate edges and extension in the overriding plate.

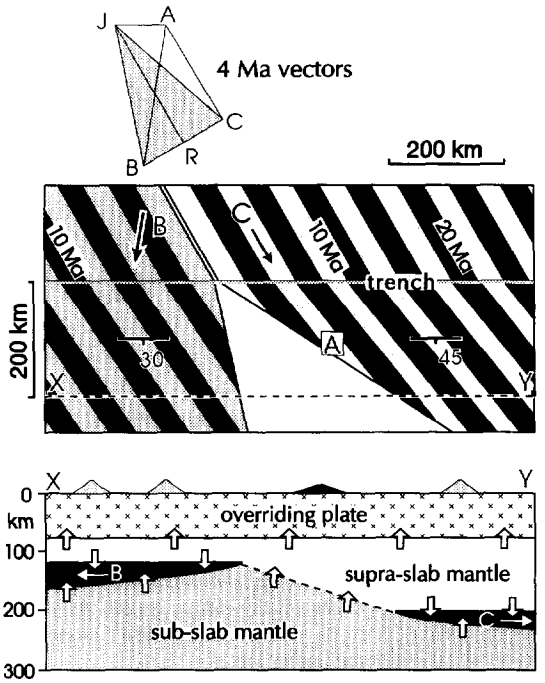

Fig. 11. Window between slabs of different dip angles. Upper two diagrams indicate relative velocities and configuration of plates. Plates *B* and *C* are descending at 30 and 45°, respectively. Subducted slabs are projected vertically onto surface of overriding plate *A*. Stripes on plates *B* and *C* represent 2 Ma of spreading. Vector lengths in velocity diagram are for 4 Ma of elapsed time. Bottom diagram is cross section *XY*, 200 km from trench. Thickness of overriding thermal lithosphere is 80 km thick; thicknesses of slabs are based on thermal model of Crough (1975), assuming no thermal erosion after subduction. Sub- and supra-slab mantle reservoirs share a planar interface in the slab window, assuming no mantle upwelling or downwelling. Flow of heat into overriding and subducted lithosphere is schematically shown by short arrows. Heat is lost from the mantle to the subducted slabs except in the slab window. A thermal anomaly in the supra-slab mantle, and possibly the overriding plate, is predicted for the slab window region. Possible arc volcanoes (grey) and slab window volcano (black) are shown schematically.

Divergence of the subducted slabs results in a loss of lithospheric volume beneath the overriding plate

which is compensated by mantle flow. In the fore-arc region the slabs are directly overlain by rigid fore-arc lithosphere, so compensatory flow is likely to be restricted to the sub-slab asthenosphere. As the asthenosphere flows upward into the narrow, near-trench window, decompression melting may occur (Presnall et al., 1979), producing melts akin to mid-ocean ridge basalts very near the trench (Bradley et al., 1995) and more alkalic magmas farther beneath the fore arc (Hole and Larter, 1993). This process, recognized by Marshak and Karig (1977) and called the "blow-torch" effect by DeLong et al. (1979), is the probable cause of modern fore-arc volcanism in the Solomon Islands (Johnson et al., 1987), late Tertiary fore-arc magmatism in Japan (Hibbard and Karig, 1990), California (Johnson and O'Neil, 1984; Fox et al., 1985) and Chile (Kaeding et al., 1990; Forsythe and Prior, 1992), and early Tertiary nearshore volcanism in Oregon and Washington (Babcock et al., 1992). Voluminous assimilation or anatexis of the fore-arc wedge may result from mafic "blow torch" magmatism, leading to emplacement of intermediate or granitic rocks. These processes are responsible for early Tertiary granitoid emplacement, gold veining, and metamorphism in a displaced fore-arc complex in Alaska (Moore et al., 1983; Sisson and Pavlis, 1993; Bradley et al., 1995; Pavlis and Sisson, 1995), and late Tertiary rhyolitic fore-arc volcanism in northern California (Johnson and O'Neil, 1984).

Inboard from the fore arc, the descending slabs are enveloped by asthenospheric mantle. In this environment, the void between the diverging slabs may be filled by upflow of sub-slab mantle, downflow of supra-slab mantle, or by combination of the two. The two mantle reservoirs come into contact with one another and possibly mix in the region of the slab window. Net upflow or downflow of mantle through the window may occur, depending on differential density, rheology, and pressure. Upflow may predominate if the sub-slab mantle is considerably hotter and less dense than the supra-slab mantle mantle, if spreading ridge convection persists after window formation (Farrar and Dixon, 1993), or if slab dip angles steepen, increasing the volume of the overlying asthenospheric wedge (Thorkelson and Taylor, 1989). In Eocene times, northeastward steepening of the southern margin of the Kula–Farallon slab window is implied by southwestward transgression of magmatism in the western United States (Thorkelson, 1995).

In principle, upflow of asthenosphere may lead to decompressional melting. Sub-slab mantle is likely to be nearly anhydrous and may undergo partial melting if it upwells significantly at depths less than about 135 km (summarized by Hole and Larter, 1993). Mixtures between sub- and supra-slab reservoirs may be partially hydrated, and prone to melt from smaller degrees of upflow, or at greater depths.

The base of the supra-slab mantle in the slab window may melt even if no mantle upflow occurs. Although the supra-slab mantle may have been metasomatized from slab dewatering, the mantle within about 30 km of the upper slab surface may have remained below its solidus because of chilling by 200–700°C (Davies and Stevenson, 1992; Peacock, 1993). In the slab window, conduction of heat from the sub-slab mantle could raise the temperature of overlying serpentinized peridotite to its melting point. For example, a region of supra-slab mantle peridotite which had been concurrently chilled and hydrated at 100 km depth could have a solidus of 1100°C and a temperature of 1050°C (Thompson, 1992), and would remain solid (Fig. 12). If this region of mantle was drawn down to 200 km depth by adiabatic corner-flow circulation induced by slab descent (Davies and Stevenson, 1992), it would obtain a temperature of about 1100°C with a solidus of about 1250°C. If this mantle flowed into a slab window at that depth, and became juxtaposed with 1450°C (normal potential temperature) sub-slab asthenosphere, the partially hydrated peridotite could be heated beyond its melting point. Depending on the specific physical, chemical and thermal history, involving cooling, hydration, reheating and possibly sub- and supra-slab asthenosphere mixing and ascent, the chemistry of the magmatic products could vary from alkalic to tholeiitic and calc-alkalic, consistent with the variety of igneous compositions expressed above slab windows (e.g., Johnson et al., 1987; Hole and Larter, 1993).

A tectonic scenario in which the foregoing situation could develop is illustrated by Fig. 12. Transfer of mantle (e.g., upwelling) through the window is considered nil, and a planar interface separates the mantle reservoirs. Mantle currents near the trailing plate edges are likely to reflect both down-dip vis-

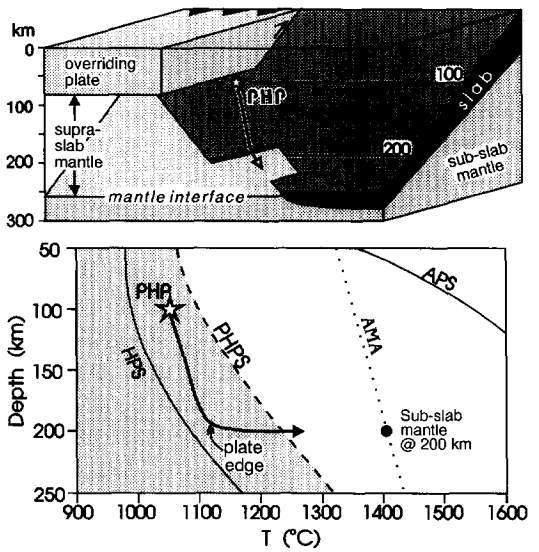

Fig. 12. Block diagram of a slab window and accompanying depth–temperature graph indicating a proposed mechanism of basaltic magma generation. Top diagram indicates possible route taken by partially hydrated peridotite (*PHP*) above descending slab near margin of slab window (only one slab shown). Peridotite flows from 100 km to 200 km depth where it crosses a former transform fault boundary, enters slab window, and comes into contact with hotter and drier sub-slab mantle. For clarity, most of the overriding plate has been cut away. Bottom diagram indicates proposed depth–temperature path of PHP. Star-marked *PHP* represents mantle which is partially hydrated and chilled from subducting slab. Shaded region is subsolidus field for this mantle composition. As mantle descends along top of slab it increases in temperature adiabatically. After flowing across plate edge into slab window, it becomes heated above partially hydrated peridotite solidus (*PHPS*) by sub-slab mantle whose temperature lies on the average mantle adiabat (*AMA*; 1300°C potential temperature). *HPS* = hydrated peridotite solidus; *APS* = anhydrous peridotite solidus; curves after Thompson (1992).

cous coupling to the slab (e.g., Peacock, 1993) and infilling of the window. Therefore, mantle above the slab is likely to flow at some angle toward the plate edge, flowing into the window at depth. The arrow in Fig. 12 illustrates a possible flow path for mantle which has been chilled and partially hydrated at 100 km depth, near the top of the slab. After flowing downward along the slab, this portion of mantle reaches the trailing plate edge at about 200 km depth, flows into contact with hotter sub-slab mantle and becomes heated.

Trace-element and isotope geochemistry indicates that mafic igneous rocks emplaced above the slab windows of the Antarctic Peninsula, British Columbia and southern California were derived largely from sub-slab or "suboceanic" asthenosphere (Bevier et al., 1979; Bevier, 1989; Forsythe and Prior, 1992; Hamilton and Dostal, 1993; Hole et al., 1995; Cole and Basu, 1995). This observation implies that asthenospheric upwelling from the sub-slab reservoir is, at least locally, a prominant mantle process. Farrar and Dixon (1993) suggested that mantle upflow induced by sea-floor spreading would continue beneath the overriding plate after ridge subduction for several million years. Whether upwelling can be sufficiently long-lived and voluminous to cause widespread basaltic volcanism hundreds of kilometres from the slab window, as they suggested, is conjectural.

Supra-slab mantle may contribute significantly to slab window magmatism, particularly along the margins of a window. Mixing of the mantle reservoirs, or their derivative magmas, is apparent from the variable arc and non-arc character of the Wrangell volcanic belt (Skulski et al., 1991) and the Alert Bay volcanic belt (Armstrong et al., 1985), which lie along the northern and southern margins, respectively, of the British Columbian slab window (Thorkelson and Taylor, 1989). Partial melting of the window margins may also be a source of volcanism. Defant and Drummond (1990) and Peacock (1991), demonstrated that young subducted lithosphere, such as the trailing plate edges of a slab window margin, are likely to partially melt. High-Mg andesites and dacites ("adakites" and "bajaites") erupted above the northern margin of the Chile slab window (Kay et al., 1993), and above remnants of the Farallon plate in Baja Mexico (Rogers and Saunders, 1989) may be products of window-margin melting.

Extensional or transtensional strain in the overriding plate is likely to develop during slab window formation. Although variations in heat flow or mantle dynamics may play a role in extension (Wilson, 1988), most of the strain is likely to result from changes in end-load stresses (Livaccari and Perry, 1993) during the transition from single-plate subduction to dual-plate subduction (or subduction and transcurrence). Partial coupling between the overriding plate and the diverging plates in the trench region will occur in different directions on opposite sides of the triple junction. If the differential stresses

brought about by the coupling are sufficiently high, the overriding lithosphere may undergo strike-slip and extensional faulting (Thorkelson and Taylor, 1989; Babcock et al., 1992; Murdie et al., 1993; Bardoux and Mareschal, 1994; Roeske et al., 1995), possibly resulting in alkalic, tholeiitic, or bimodal magmatism. Thus, igneous activity in the general region of a slab window may be an expression of both lithospheric and asthenospheric processes.

4.2. Magmatic effects of a migrating slab window

A sequence of possible magmatic effects produced by migration of a slab window below a 900 × 350 km area of overriding plate A is illustrated in Fig. 13. Where subducted, oceanic plate B is dipping at 25°, and plate C, with its smaller velocity of convergence, is dipping at 50°. The triple junction and corresponding slab window are migrating rapidly southward at 100 km/Ma (10 cm/a), as indicated by vector AJ in velocity space. This situation is broadly analogous to the tectonic environment of the Chile slab window (Forsythe and Nelson, 1985; Ramos and Kay, 1992; Murdie et al., 1993).

Initially, the triple junction (J) is located in the northern part of the trench, and most of overriding plate A overlies the gently dipping subducted slab of plate B (Fig. 13a). A calc-alkaline volcanic arc on overriding plate A is active between the 100 km and 150 km structure contours on the upper surface of slab B (cf. Gill, 1981). After 3.5 Ma of elapsed time (Fig. 13b), the triple junction and slab window have

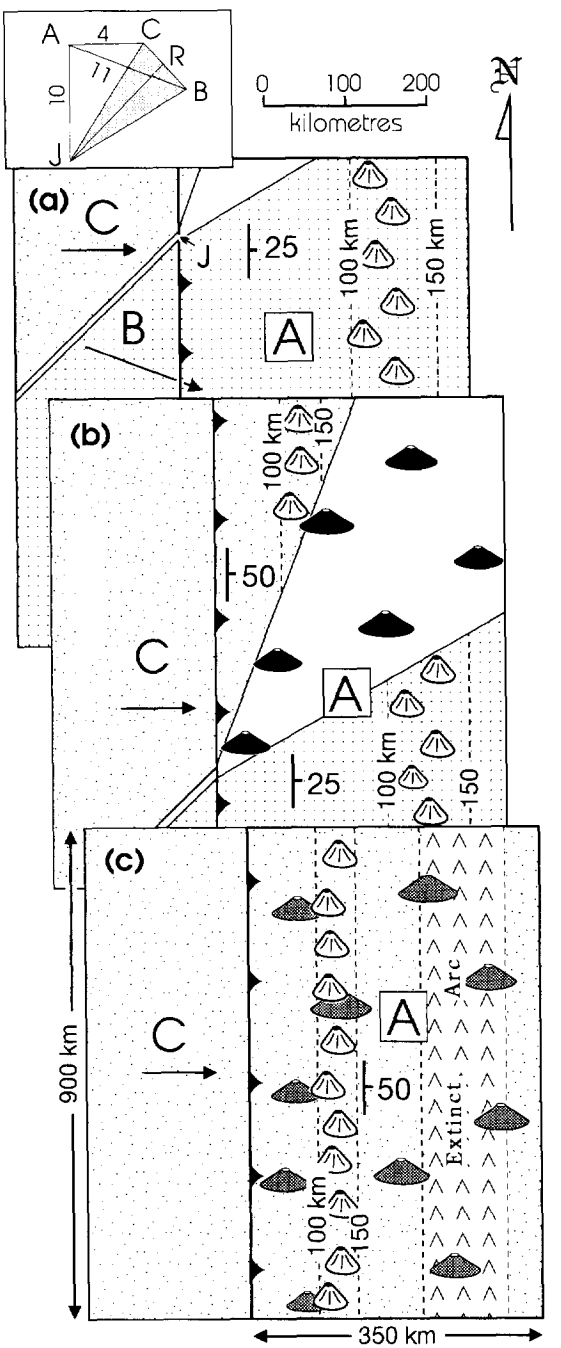

Fig. 13. Possible magmatic effects from migration of a slab window beneath a 350×900 km area of plate *A*. Plate *B* is converging rapidly (11 cm/a) at 30° from orthogonal, whereas plate *C* is converging orthogonally at a slower rate (4 cm/a), as indicated in the velocity diagram. In (a), a slab window appears beneath the northern part of the area. Ridge orientation and plate motions require southward migrating triple junction and slab window. Most of the area of plate *A* is underlain by subducted parts of plate *B*, which is descending into the asthenosphere with 25° dip. A volcanic arc on plate *A* is active between the 100 and 150 km depth contours of the subducted slab. In (b) the slab window has migrated southward, underlying much of plate *A*. Tholeiitic to alkalic volcanoes (black) have formed above the window. Plate *C*, dipping at 50°, now underies much of the northern area of plate *A*, resulting in formation of a narrow, near-trench arc. In (c) the window has migrated to the south, and the area records a three-stage magmatic chronolgy. The arc previously generated above plate *B* became extinct (∧ pattern) and succeeded by "slab window" volcanoes that are waning or extinct (grey), which in turn have been superseded by calc-alkaline volcanoes forming an active arc above subducting slab *C*.

migrated about 350 km southward, leading to major changes in magmatic regime. The northern part of the volcanic arc (originally built above slab B) is underlain by the slab-free region, and calc-alkaline volcanism has given way to alkalic or tholeiitic eruptions. The volcanic activity, collectively termed *slab window volcanism*, may have a broader distribution than the arc volcanism, extending from fore-arc to retro-arc regions. Extensional or transtensional faulting and concomitant uplift locally control the distribution of the slab window volcanism. If slab window magmatism is voluminous, and plate forces are appropriate (Cross and Pilger, 1982), the overriding plate may become highly attenuated, leading to rifting and back-arc basin development (cf., Tamaki, 1985; Farrar and Dixon, 1993). As the triple junction migrates southward, subduction of the ridge crest may produce variable contraction, transcurrence, uplift and subsidence in the fore arc (Corrigan et al., 1990; Forsythe and Prior, 1992).

As the slab window migrates southward, plate C progressively replaces plate B as the subducting slab. Consequently, a new calc-alkaline arc has formed on the northern part of plate A. This new arc is narrower and closer to the trench than the arc above plate B, because plate C is descending more steeply than plate B. Initially, the newly formed parts of the arc above plate C may inherit some "rift" or otherwise anomalous chemical characteristics from lingering magmas produced by passage of the slab window, but as the window migrates farther southward the arc should develop typical arc geochemical character. Thus, southward migration of the slab window is accompanied by progressive extinction of the volcanic arc of plate B, and synchronous southward lengthening of the arc above plate C. This diachronous, trenchward transition of arc volcanism from arc B to arc C is temporally linked to a southward sweep of slab window magmatic activity.

After another 12 Ma of elapsed time (Fig. 13c), the slab window has migrated southward beyond the study area, and only plate C is subducting. An idealized three-stage chronology of volcanic activity on plate A is presented. The oldest volcanic rocks are those produced in the volcanic arc which was generated when plate B was being subducted. Locally overlying this extinct arc are younger volcanic rocks attributed to slab window magmatism. These volcanoes, particularly those close to the trench, may become extinct after passage of the slab window, or may continue to be active for millions of years as back-arc volcanoes (cf. Ramos and Kay, 1992) particulary if the overriding plate is under tension. Assuming eventual termination of the slab window volcanism, the youngest volcanic rocks will be those produced by subduction of plate C. The steeper angle of dip of plate C has resulted in a trenchward jump in the axis of arc volcanism. If alkalinity in the arcs increases away from the trench (Hatherton and Dickinson, 1969), then the overall arc complex, consisting of both the extinct and the active arcs, would be expected to show repetition of across-arc alkalinity trends (Thorkelson, 1990).

5. Conclusions

Convergent and divergent plate margins are the most important sites of lithospheric rejuvenation. Development of volcanic arcs at convergent margins and formation of new oceanic crust at divergent margins are well understood, and their main geophysical and magmatic signatures are documented. In contrast, the special environments in which convergent and divergent plate boundaries intersect have been less comprehensively characterized.

Several ridge–trench encounters in the Pacific region have occurred since Late Cretaceous times. Considered together, they provide a general understanding of how a spreading ridge may behave as it approaches a subduction zone. In some tectonic regimes, the ridge may stall or pivot as the bounding plates break up in response to increasing buoyancy and decreasng strength. In other situations, however, the ridge may maintain its orientation and integrity, and the bounding plates may subduct uniformly. Under these conditions, slab continuity is preserved and the slabs separate beneath the overriding plate in a predictable manner. The divergent margin is progressively unzipped, forming a slab window. Simple geometrical procedures can be applied to estimate slab window shapes and sizes.

The development of slab windows beneath convergent margins should be considered an essential part of plate tectonic theory. The episodic effects of slab window formation and migration should be

expected in a significant proportion of volcanic arcs. In the interpretation of ancient arc systems, "ridge subduction" should be considered a likely cause of anomalous magmatic and tectonic events, particularly those involving features such as fore-arc volcanism, alkaline or tholeiitic magmas, uplift and extensional tectonism.

Despite the importance of slab windows to the evolution of convergent plate margins, few principles governing their geometry have been previously determined. Those provided in this paper outline the styles expected from simple plate kinematics for a variety of ridge–transform–trench configurations. However, more comprehensive models, involving factors such as thermal erosion, spherical shell strain, and non-uniform spreading and subduction, are necessary to provide an improved foundation for the realistic depiction of slab windows. More sophisticated models will permit an advanced understanding of how slab windows affect the overriding lithosphere under variable physical, chemical and thermal conditions.

Acknowledgements

In the development of the ideas expressed in this paper, the author benefited from the encouragement and challenging comments of Stephen Johnston, Bradford Johnson, Richard Taylor, Robin Riddihough, David Engebretson, Scott Babcock, Ted Irving and Craig Hart. Peter Lonsdale and Peter Ward made suggestions on an earlier version. Will van Randen helped with computer drafting. Journal referees Malcolm Hole and Edward Farrar are thanked for constructive reviews.

References

Armstrong, R.L., Muller, J.E., Harakal, J.E. and Muehlenbachs, K., 1985. The Neogene Alert Bay volcanic belt of northern Vancouver Island, Canada: Descending-plate-edge volcanism in the arc–trench gap. J. Volcanol. Geotherm. Res., 26: 75–97.

Atwater, T.M., 1970. Implications of plate tectonics for the Cenozoic tectonic evolution of western North America. Geol. Soc. Am. Bull., 81: 3513–35.

Atwater, T. and Severinghaus, J., 1989. Tectonic maps of the northeast Pacific. In: E.L. Winterer, D.M. Hussong and R.W. Decker (Editors), The Eastern Pacific Ocean and Hawaii. (The Geology of North America, Vol. N.) Geol. Soc. Am., Boulder, CO, pp. 15–20.

Babcock, S., Burmester, R.F., Engebretson, D.C., Warnock, A. and Clark, K.P., 1992. A rifted margin origin for the Crescent Basalts and related rocks in the northern Coast Range volcanic province, Washington and British Columbia. J. Geophys. Res., 97: 6799–6821.

Bardoux, M. and Mareschal, J.-C., 1994. Extension in south-central British Columbia: mechanical and thermal controls. Tectonophysics, 238: 451–470.

Bevier, M.L., 1989. A lead and strontium isotopic study of the Anahim volcanic belt, British Columbia: Additional evidence for widespread suboceanic mantle beneath western North America. Geol. Soc. Am. Bull., 101: 973–981.

Bevier, M.L., Armstrong, R.L. and Souther, J.G., 1979. Miocene peralkaline volcanism in west-central British Columbia — its temporal and plate-tectonics setting. Geology, 7: 389–392.

Bird, P., 1988. Formation of the Rocky Mountains, western United States: A continuum computer model. Science, 239: 1501–1507.

Bradley, D., Haeussler, P., Nelson, S., Kusky, T., Donley, D.T. and Goldfarb, R., 1995. Geological effects of Paleogene ridge subduction, Kenai Peninsula, southern Alaska. Geol. Soc. Am., Cordilleran Sect., 27: 7.

Cande, S.C., Leslie, R.B., Parra, J.C. and Hobart, M., 1987. Interaction between the Chile ridge and Chile trench: Geophysical and geothermal evidence. J. Geophys. Res., 92: 495–520.

Cloos, M., 1993. Lithospheric buoyancy and collisional orogenesis: Subduction of oceanic plateaus, continental margins, island arcs, spreading ridges, and seamounts. Geol. Soc. Am. Bull., 105: 715–737.

Cole, R.B. and Basu, A.R., 1995. Nd-Sr isotopic geochemistry and tectonics of ridge subduction and middle Cenozoic volcanism in western California. Geol. Soc. Am. Bull., 107: 167–179.

Corrigan, J., Mann, P. and Ingle Jr., J.C., 1990. Forearc response to subduction of the Cocos Ridge, Panama–Costa Rica. Geol. Soc. Am. Bull., 102: 628–652.

Cross, T.A. and Pilger, R.H., 1982. Controls of subduction geometry, location of magmatic arcs, and tectonics of arc and back-arc regions. Geol. Soc. Am., 93: 545–562.

Crough, S.T., 1975. Thermal model of oceanic lithosphere. Nature, 256: 388–390.

Davies, J.H. and Stevenson, D.J., 1992. Physical model of source region of subduction zone volcanics. J. Geophys. Res., 97: 2037–2070.

Defant, M.J. and Drummond, M.S., 1990. Derivation of some modern arc magmas by melting of young subducted lithosphere. Nature, 347: 662–665.

DeLong, S.E. and Fox, P.J., 1977. Geological consequences of ridge subduction. In: M. Talwani and W.C. Pitman III (Editors), Island Arcs, Deep Sea Trenches and Back-arc Basins. Am. Geophys. Union, Maurice Ewing Ser., 1: 221–228.

DeLong, S.E., Fox, P.J. and McDowell, F.W., 1978. Subduction of the Kula Ridge at the Aleutian Trench. Geol. Soc. Am. Bull., 89: 83–95.

DeLong, S.E., Schwarz, W.M. and Anderson, R.N., 1979. Thermal effects of ridge subduction. Earth Planet. Sci. Lett., 44: 239–246.

Dickinson, W.R. and Snyder, W.S., 1978. Plate tectonics of the Laramide orogeny. In: V. Matthews III (Editor), Laramide Folding Associated with Basement Block Faulting in the Western United States. Geol. Soc. Am. Mem., 151: 355–6.

Dickinson, W.R. and Snyder, W.S., 1979. Geometry of subducted slabs related to San Andreas transform. J. Geol., 87: 609–627.

Dixon, J.M. and Farrar, E., 1980. Ridge subduction, eduction, and the Neogene tectonics of southwestern North America. Tectonophysics, 67: 81–99.

Farrar, E. and Dixon, J.M., 1993. Ridge subduction: kinematics and implications for the nature of mantle upwelling. Can. J. Earth Sci., 30: 893–907.

Forsythe, R.D. and Nelson, E.P., 1985. Geological manifestations of ridge collision: evidence from the Golfo de Penas–Taitao Basin, southern Chile. Tectonics, 4: 477–495.

Forsythe, R.D. and Prior, R., 1992. Cenozoic continental geology of South America and its relations to the evolution of the Chile triple junction. Proc. ODP Sci. Results, 141: 23–31.

Fox, K.F., Fleck, R.J., Curtis, G.H. and Meyer, C.E., 1985. Implications of the northwestwardly younger age of the volcanic rocks of west-central California. Geol. Soc. Am., 96: 647–654.

Gasparik, T., 1993. The role of volatiles in the transition zone. J. Geophys. Res., 98: 4287–4299.

Gill, J.B., 1981. Orogenic Andesites and Plate Tectonics. Springer, Berlin, 390 pp.

Hamilton, T.S. and Dostal, J., 1993. Geology, geochemistry, and petrogenesis of Middle Tertiary volcanic rocks of the Queen Charlotte Islands, British Columbia (Canada). J. Volcanol. Geotherm. Res., 59: 77–99.

Hatherton, T. and Dickinson, W.R., 1969. The relationship between andesitic volcanism and seismicity in Indonesia, the Lesser Antilles, and other island arcs. J. Geophys. Res., 74: 5301–5310.

Herron, E.M., Cande, S.C. and Hall, B.R., 1981. An active spreading center collides with a subduction zone: a geophysical survey of the Chile margin triple junction. In: L.D. Kulm, J. Dymond, E.J. Dasch, D.M. Hussong and R. Roderick (Editors), Nazca Plate: Crustal Formation and Andean Convergence. Geol. Soc. Am. Mem., 154: 683–701.

Hibbard, J.P. and Karig, D.E., 1990. Structural and magmatic responses to spreading ridge subduction: an example from southwest Japan. Tectonics, 9: 207–230.

Hole, M.J., 1988. Post-subduction alkaline volcanism along the Antarctic Peninsula. J. Geol. Soc. London, 145: 985–998.

Hole, M.J. and Larter, R.D., 1993. Trench-proximal volcanism following ridge crest–trench collision along the Antarctic Peninsula. Tectonics, 12: 897–910.

Hole, M.J., Rogers, G., Saunders, A.D. and Storey, M., 1991. Relation between alkalic volcanism and slab window formation. Geology, 19: 657–660.

Hole, M.J., Saunders, A.D., Rogers, G. and Sykes, M.A., 1995. The relationship between alkalic magmatism, lithospheric extension and slab window formation along continental destructive plate margins. In: J.L. Smellie (Editor), Volcanism Associated with Extension along Consuming Plate Margins. Geol. Soc. London Spec. Publ., 81: 265–285.

Irifune, T. and Ringwood, A.E., 1993. Phase transformations in subducted oceanic crust and buoyancy relationships at depths of 600–800 km in the mantle. Earth Planet. Sci. Lett., 117: 101–110.

Isacks, B.L. and Barazangi, M., 1977. Geometry of Benioff zones: Lateral segmentation and downwards bending of the subducted lithosphere. In: M. Talwani and W.C., Pitman III (Editors), Island Arcs Deep Sea Trenches and Back-arc Basins. Am. Geophys. Union, Maurice Ewing Ser., 1: 99–114.

Johnson, C.M. and O'Neil, J.R., 1984. Triple junction magmatism: a geochemical study of Neogene volcanic rocks in western California. Earth Planet. Sci. Lett., 71: 241–262.

Johnson, R.W., Jaques, A.L., Langmuir, C.H., Perfit, M.R., McColloch, M.T., Staudigel, H., Chapell, B.W. and Taylor, S.R., 1987. Ridge subduction and fore-arc volcanism: petrology, and geochemistry of rocks dredged from the western Solomon arc and Woodlark Basin. In: B. Taylor and N. Exon (Editors), Marine Geology, Geophysics and Geochemistry of the Woodlark Basin — Solomon Islands. Circum-Pac. Counc. Energy Miner. Resour., Earth Sci. Ser., 7: 113–154.

Kaeding, M., Forsythe, R.D. and Nelson, E.P., 1990. Geochemistry of the Taitao ophiolite and near-trench intrusions from the Chile margin triple junction. J. S. Am. Earth Sci., 3: 161–177.

Kay, S.M., Ramos, V.A. and Marquez, M., 1993. Evidence in Cerro Pampa volcanic rocks for slab-melting prior to ridge–trench collision in southern South America. J. Geol., 101: 703–714.

Larter, R.D. and Barker, P.F., 1991. Effects of ridge crest–trench interaction on Antarctic–Phoenix spreading: Forces on a young subducting plate. J. Geophys. Res., 96: 19,583–19,607.

Livaccari, R.F. and Perry, F.V., 1993. Isotopic evidence for preservation of Cordilleran lithospheric mantle during the Sevier–Laramide orogeny, western United States. Geology, 21: 719–722.

Luyendyk, B.P., 1995. Hypothesis for Cretaceous rifting of east Gondwana caused by slab capture. Geology, 23: 373–376.

Marshak, R.S. and Karig, D.E., 1977. Triple junctions as a cause for anomalously near-trench igneous activity between the trench and volcanic arc. Geology, 5: 233–2.

McKenzie, D.P., 1969. Speculations on the consequences and causes of plate motions. Geophys. J. R. Astron. Soc., 18: 1–32.

McKenzie, D.P. and Morgan, J.W., 1969. Evolution of triple junctions. Nature, 224: 125–133.

Menard, H.W., 1978. Fragmentation of the Farallon plate by pivoting subduction. J. Geol., 86: 99–110.

Moore, J.C., Byrne, T., Plumley, P.W., Reid, M., Gibbons, H. and Coe, R.S., 1983. Paleogene evolution of the Kodiak Islands, Alaska: Consequences of ridge–trench interaction in a more southerly latitude. Tectonics, 2: 265–293.

Murdie, R.E., Priior, D.J., Styles,P., Flint, S.S., Pearce, R.G. and Agar, S.M., 1993. Seismic responswes to ridge-transform subduction: Chile triple junction. Geology, 21: 1095–1098.

Palmer, H., 1968. East Pacific rise and westward drift of North America. Nature, 220: 341–345.

Pavlis, T.L. and Sisson, V.L., 1995. Structural history of the Chugach Metamorphic Complex in the Tana River region, eastern Alaska: A record of Eocene ridge subduction. Geol. Soc. Am. Bull., 107: 1333–1335.

Peacock, S.M., 1991. Numerical simulation of subduction zone pressure–temperature–time paths: constraints on fluid production and arc magmatism. Philos. Trans. R. Soc. London, Ser. A., 335: 341–353.

Peacock, S.M., 1993. Large-scale hydration of the lithosphere above subducting slabs. Chem. Geol., 108: 49–59.

Presnall, D.C., Dixon, J.R., O'Donnell, T.H. and Dixon, S.A., 1979. Generation of mid-ocean ridge tholeiites. J. Petrol., 20: 3–35.

Ramos, V.A. and Kay, S.M., 1992. Southern Patagonian plateau basalts and deformation: backarc testimony of ridge collision. Tectonophysics, 205: 261–282.

Riddihough, R.P., 1984. Recent movements of the Juan de Fuca plate system. J. Geophys. Res., 89: 6980–6994.

Roeske, S.M., Snee, L.W., Pavlis, T.L. and Sisson, V.B., 1995. Tectonic response of the Chugach accretionary comlex to Early Cenozoic oblique subduction. Geological effects of Paleogene ridge subduction, Kenai Peninsula, southern Alaska. Geol. Soc. Am., Cordilleran Sect., 27: 74.

Rogers, G. and Saunders, A.D., 1989. Magnesian andesites from Mexico, Chile and the Aleutian Islands: Implications for magmatism associated with ridge–trench collisions. In: A.J. Crawford (Editor), Boninites and Related Rocks. Unwin Hyman, London, pp. 416–445.

Severinghaus, J. and Atwater, T., 1990. Cenozoic geometry and thermal state of the subducting slabs beneath western North America. In: B.P. Wernicke (Editor), Basin and Range Extensional Tectonics near the Latitude of Las Vegas, Nevada. Geol. Soc. Am. Mem., 176: 1–22.

Sisson, V.B. and Pavlis, T.L., 1993. Geological consequences of plate reorganization: An example from the Eocene southern Alaska fore arc. Geology, 21: 913–916.

Sisson, V.B., Pavlis, T.L. and Prior, D.J., 1994. Effects of triple junctions at convergent plate margins. GSA Today, October: 248–249.

Skulski, T., Francis, D. and Ludden, J., 1991. Arc-transform magmatism in the Wrangell volcanic belt. Geology, 19: 11–14.

Stock, J. and Molnar, P., 1988. Uncertainties and implications of the Late Cretaceous and Tertiary position of North America relative to the Farallon, Kula, and Pacific plates. Tectonics, 7: 1339–1384.

Tamaki, K., 1985. Two modes of back-arc spreading. Geology, 13: 475–478.

Thompson, A.B., 1992. Water in the Earth's upper mantle. Nature, 358: 295–302.

Thompson, R.N., Morrison, M.A., Hendry, G.L. and Parry, S.J., 1984. An assessment of the relative roles of crust and mantle in magma genesis: an elemental approach. Philos. Trans. R. Soc. London, Ser. A, 310: 549–590.

Thorkelson, D.J., 1990. Tectonic and magmatic aspects of slab windows. Geol. Assoc. Can., Progr. Abstr., 15: A131.

Thorkelson, D.J., 1994. Ridge subduction: kinematics and implications for the nature of mantle upwelling: Discussion. Can. J. Earth Sci., 31: 1486–1489.

Thorkelson, D.J., 1995. The Paleogene Kula–Farallon slab window. Geol. Assoc. Can., Progr. Abstr., 20: A105.

Thorkelson, D.J. and Taylor, R.P., 1989. Cordilleran slab windows. Geology, 17: 833–8.

Uyeda, S. and Miyashiro, A., 1974. Plate tectonics and the Japanese Islands: A synthesis. Geol. Soc. Am. Bull., 85: 1159–1170.

Van den Beukel, 1990. Breakup of young oceanic lithosphere in the upper part of a subduction zone: implications for the emplacement of ophiolites. Tectonics, 9: 825–844.

Van der Hilst, R. and Seno, T., 1993. Effects of relative plate motions on the deep structure and penetration depth of slabs below the Izu–Bonin and Mariana island arcs. Earth Planet. Sci. Lett., 120: 395–407.

Van der Hilst, R., Engdahl, R., Spakman, W. and Nolet, G., 1991. Tomographic imaging of subducted lithosphere below northwest Pacific island arcs. Nature, 353: 37–43.

Weissel, J.K., Taylor, B. and Karner, G.D., 1982. The opening of the Woodlark Basin, subduction of the Woodlark spreading system, and the evolution of northern Melanesia since mid-Pliocene time. Tectonophysics, 87: 253–277.

Wilson, J.T., 1988. Convection tectonics: Some possible effects upon the Earth's surface of flow from the deep mantle. Can. J. Earth Sci., 25: 1199–1208.

Yamaoka, K. and Fukao, Y., 1986. Spherical shell tectonics. Rev. Geophys., 24: 27–53.

Zhou, H., 1990. Mapping of P-wave slab anomalies beneath the Tonga, Kermadec and New Hebrides arcs. Phys. Earth Planet. Inter., 61: 199–229.